Journal of Engineering Technology Vol. 1: 38-45, 2011
ISSN 2231-8798

Performance Analysis of Power and Spectrum Efficiency in Uplink LTE System

Z. Mansor & A.K.M. Isa
Section of Telecommunication Technology
Universiti Kuala Lumpur British Malaysian Institute
Batu 8, Jalan Sungai Pusu, 53100 Gombak, Selangor, Malayisa

Corresponding email: zuhanis@bmi.unikl.edu.my

Abstract: Less power consumption improves the battery life for mobile handsets, or could give rise to extra transmission range extension for the same mean transmitting power. The low peak-to-average power ratio (PAPR) in single- carrier systems has motivated the Long Term Evolution (LTE) Third Generation Partnership Project (3GPP) to adopt single carrier frequency division multiple access (SC-FDMA) as the uplink multiple access scheme. System performance is evaluated in terms of bit error rate, packet error rate and peak average power ratio (PAPR). In this paper, an overview of SC-FDMA standards is presented together with software simulated physical layer performance results for each of the transmission modes defined in the 3GPP LTE standard. Furthermore, we show that by applying pulse shaping in frequency domain SC-FDMA signal, the PAPR of a localized SC-FDMA signal can be further reduced at the expense of degraded spectrum efficiency. Simulation results show that a PAPR reduction of 1.9 dB can be achieved when a root-raised cosine spectrum shaping filter with a roll-off factor of 0.5 is applied. This PAPR reduction can be used to enhance the power efficiency of the handset, or alternatively to improve uplink spectrum efficiency in LTE system.

Keywords: SC-FDMA**,** PAPR, pulse shaping, root-raised cosine.

1.0 INTRODUCTION

Fourth generation (4G) systems are currently in development around the world [1]. They are largely motivated by the increasing demand for high-quality digital communications at continually increasing data rates. Bandwidth efficiency is a measure of how efficiently the allocated bandwidth is utilized in a wireless communications system. LTE is designed to meet the user needs for high-speed data. It provides uplink rates of up to 50 Megabits per second (Mbps) and downlink rates of up to 100 Mbps [2]. The multiple access scheme in the LTE uplink uses Single Carrier Frequency Division Multiple Access (SC-FDMA). The downlink uses Orthogonal Frequency Division Multiple Access (OFDMA). Significantly, these multiple access solutions provide orthogonality between the users in a common cell, thus improving network capacity by avoiding intra-cell interference.

SC-FDMA is a combination of single carrier modulation, orthogonal frequency multiplexing, and frequency domain equalization (FDE) [3]. It exhibits the key advantage of a low peak-to-average power ratio (PAPR). SC-FDMA also provides the multipath resistance and flexible sub-carrier frequency allocation offered by OFDMA. Pulse shaping is required for single-carrier systems to bandlimit the transmit signal. It plays an important role in spectrum shaping in the modern wireless communication to reduce spectrum bandwidth. A critical analysis was carried out in [4] on pulse shape filtering in wireless communication. It has shown that the pulse shaping filter not only reduces inter-symbol interference (ISI), but it also reduced adjacent channel interference. The SC-FDMA uplink requires pulse shaping to limit ISI between neighboring time symbols [5]. Pulse-shaped SC-FDMA was investigated in [6] and further studies have considered the impact of subcarrier allocation.

Battery life is another key factor that affects all mobile handsets. Even though battery technology is improving, it is important to ensure that mobiles use as little energy as possible. Signals that have a high peak to average power ratio, and thus require linear amplification, do not lend themselves easily to power efficient RF amplifications [7]. As a result it is desirable to reduce the PAPR for energy limited transmissions. Unfortunately OFDM has a high peak to average power ratio. While this is not a problem at the base station, where power is freely available, it is unacceptable at the mobile handset. However, it is still of

research and practical interest to further reduce the PAPR in SC-FDMA system. In this paper, we extend the analysis of power and bandwidth efficiency by considering the frequency domain spectrum shaping in SC-FDMA signal.

The rest of the paper is laid out as follows. In section 2, the simulation parameters and assumptions are presented. Section 3 describes the system model of SC-FDMA. Frequency domain spectrum shaping is presented in Section 4. Simulation results are given in section 5, which show PER against SNR for different transmission modes and peak to power ratio. Section 6 concludes the paper.

2.0 PARAMETER ASSUMPTIONS

Otherwise stated, the numerical values for the SC-FDMA parameters used in this paper are based on the latest 3GPP TR 36.8414 standard [9] as given in Table 1. SC-FDMA has been adopted as the uplink transmission scheme in the 3GPP LTE standard [8]. In order to investigate the link level performance of the LTE uplink, a baseband LTE link level simulator was implemented in MATLAB.

Table 1: SC-FDMA Parameters.

Carrier Frequency	2 GHz
Transmission Bandwidth	10 MHz
Time Slot/Sub Frame Duration	0.5 ms /1 ms
Subcarrier Spacing	15 kHz
Sampling Frequency	15.36 MHz
Total number of Subcarrier	1024
Number of subcarrier per user	128
Number of occupied subcarrier	600
Number of SC-FDMA symbols	7
CP Length (μs/samples) Short	(5.21/80) x 1
Channel Knowledge	Perfect
Pulse Shaping Filter	Root-Raised Cosine
Oversampling Factor	4
Roll-off Factor, α	0.5
Subcarrier Mapping Schemes	LFDMA

Table 2: Modulation and Coding Schemes (MCS) Parameters.

Mode	1	2	3	4	5	6
Modulation	QPSK		16-QAM		64-QAM	
Coding rate	1/2	3/4	1/1	3/4	1/2	3/4
Coded bits per subcarrier	2	2	4	4	6	6
Coded bits per Symbol	144	144	288	288	432	432
Coded data per Symbol	72	108	144	216	216	324
Nominal Bit Rate (Mbps)	8.4	12.6	16.8	25.2	25.21	37.8

An LTE FDD system with 10 MHz bandwidth is assumed. In the simulation, only six MCS levels are considered as shown in Table 2. PHY layer BER, PER and throughput are used as the main metric for comparison. A packet size of 54 bytes is considered. A target PER of 10% or less was assumed. In order to measure the PAPR of the *i*-th transmission block, the complementary cumulative distribution function (CCDF) is used as defined in Eq. (1).

$$P_{PAPR}(i) = 10\log\left\{\frac{\max_{t}\{|x_{tx}(t,i)|^2\}}{E[|x_{tx}(t,i)|^2]}\right. \quad (1)$$

$PAPR_0$ represents a PAPR threshold and $\max_{t}\{|x_{tx}(t,i)|^2\}$ is the peak transmit signal power. $E[|x_{tx}(t,i)|^2]$ is the average transmit signal power. The PAPR is compared against the above threshold to determine how often it is exceeded. We then plot the Complementary Cumulative Density Function (CCDF) against the $PAPR_0$ threshold. A threshold probability of 0.1% $\{\Pr\{PAPR > PAPR_0\} = 10^{-3}\}$ is used. This probability represents the 99.9-percentile PAPR, and is donated as PAPR 99.9%.

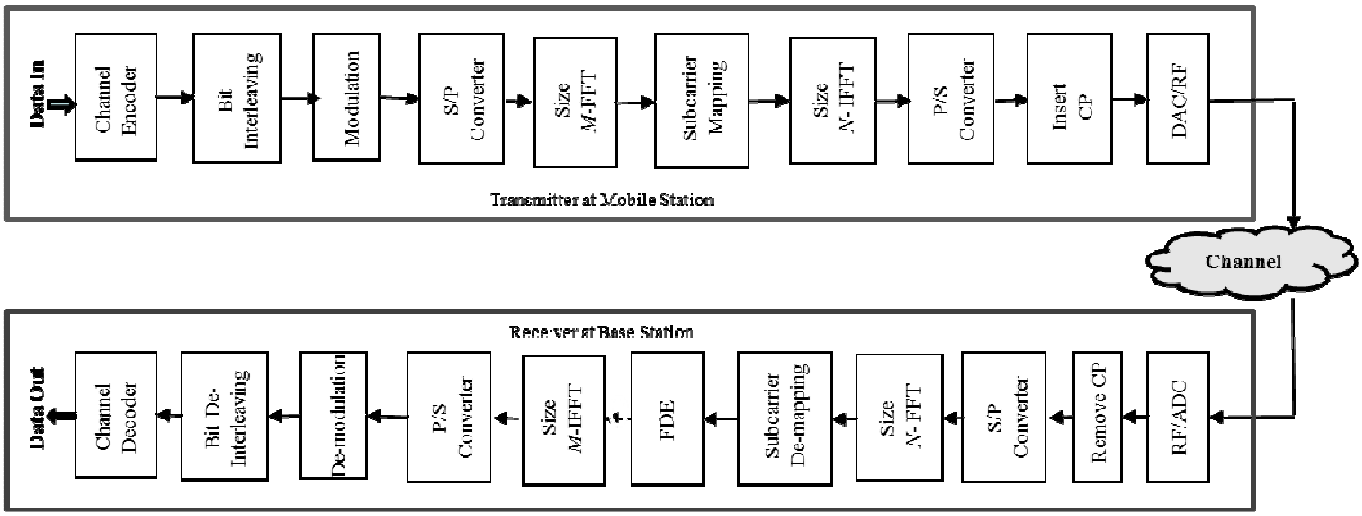

Fig. 1 SISO model of a coded SC-FDMA system.

3.0 SYSTEM MODEL

3GPP LTE uses SC-FDMA to achieve multiple access [1]. A block diagram of a single antenna SC-FDMA system is illustrated in Fig. 1. SC-FDMA can be thought of as a form of modified OFDMA for uplink transmission [8]. For the k-th user ($k = 1,2,....,Q$), the input bit stream symbol is passed through a bit-to-symbol mapping process. The M_s data symbol sequence is then grouped into blocks of size x_m. These data blocks are transformed into the frequency domain using an M-point FFT, leading to $\mathbf{X}_m = F_M x_m$ as in Eq. (2).

$$\mathrm{FFT}\{x_m\} = X_m^{(k)} = \frac{1}{\sqrt{M}} \sum_{n=0}^{M-1} x_m e^{-j\frac{2\pi}{M}nm} \qquad (2)$$

with $n, m = 1,2,.....,M$. $\mathbf{F}_M$ represents the normalized $M \times M$ FFT matrix. The data symbols from the FFT are then mapped/permuted across the entire channel spectrum, where $N > M$ and $N = Q'M$. Here Q' is an integer that represents the spreading factor. It is commonly known as the symbol bandwidth expansion factor. This is effectively the number of simultaneous users that the system can support in a single SC-FDMA symbol [16]. Since wireless communication systems are susceptible to multipath components, a cyclic prefix (CP) is added into each transmitted block prior to transmission to remove ISI. As shown in Fig. 2, the CP is a repetition of the last part of the symbol which is then added as a prefix to the start of the symbol. Although this is performed at the expense of transmission bandwidth, the CP prevents interference from previously transmitted blocks due to multipath delay spread and hence maintains orthogonality between the subcarriers.

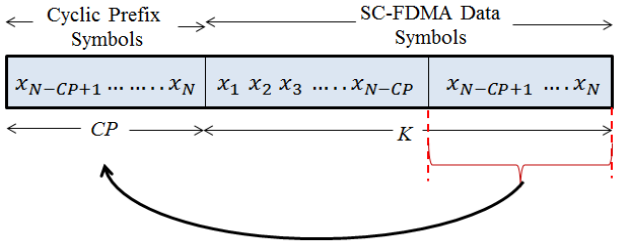

Fig. 2: Block diagram of Cyclic Prefix insertion.

$$y(t) = x(t) * h(t) \qquad (3)$$

The SC-FDMA symbol in the time domain of length N vector

$$\mathbf{x} = [x_1\ x_2\ x_3\ .....\ x_N]^T \qquad (4)$$

The channel is known by a channel impulse response (CIR) where

$$\mathbf{h} = [h_1\ h_2\ h_3\ .....\ h_L]^T \qquad (5)$$

and contains L equally spaced time-domain taps. Thus,

$$\mathbf{y} = \mathbf{h} \otimes \mathbf{x} \qquad (6)$$

$$y_1 = x_{1,2}h_0 + x_{P,1}h_1 + x_{P-1,1}h_2 + ... + x_{P-CP+1,1}h_L$$

$$y_2 = x_{2,2}h_0 + x_{1,2}h_1 + x_{P,1}h_2 + x_{P-1,1}h_3 + ... + x_{P-CP+2,2}$$

$$y = \begin{bmatrix} y_1 \\ y_2 \\ \vdots \\ \vdots \\ \vdots \\ y_P \end{bmatrix} = \begin{bmatrix} 0 & \dots & 0 & h_L & \cdots & h_2 & h_1 \\ 0 & \ddots & \ddots & 0 & h_L & & h_2 \\ \vdots & \ddots & \ddots & \ddots & 0 & \ddots & \vdots \\ \vdots & \ddots & \ddots & \ddots & \ddots & \ddots & h_L \\ \vdots & \ddots & \ddots & \ddots & \ddots & \ddots & 0 \\ \vdots & \ddots & \ddots & \ddots & \ddots & \ddots & \vdots \\ 0 & \cdots & \cdots & \cdots & \cdots & 0 & 0 \end{bmatrix} \begin{bmatrix} x_{1,1} \\ x_{2,1} \\ \vdots \\ x_{P-CP+1,1} \\ x_{P-CP+2,1} \\ \vdots \\ x_{P,1} \end{bmatrix} + \begin{bmatrix} h_0 & 0 & 0 & \cdots & \cdots & \cdots & 0 \\ h_1 & h_0 & \ddots & \ddots & \ddots & \ddots & 0 \\ \vdots & h_1 & \ddots & \ddots & \ddots & \ddots & \vdots \\ h_L & \vdots & \ddots & \ddots & \ddots & \ddots & \vdots \\ 0 & h_L & \ddots & \ddots & \ddots & \ddots & \vdots \\ \vdots & \ddots & \ddots & \ddots & \ddots & \ddots & 0 \\ 0 & \cdots & 0 & h_L & \cdots & h_1 & h_0 \end{bmatrix} \begin{bmatrix} x_{1,2} \\ x_{2,2} \\ \\ x_{P-CP+1,2} \\ x_{P-CP+2,2} \\ \vdots \\ x_{P,2} \end{bmatrix} \quad (7)$$

$$\mathbf{y} = \mathbf{H}_1\mathbf{x}_1 + \mathbf{H}_0\mathbf{x}_2 \quad (8)$$

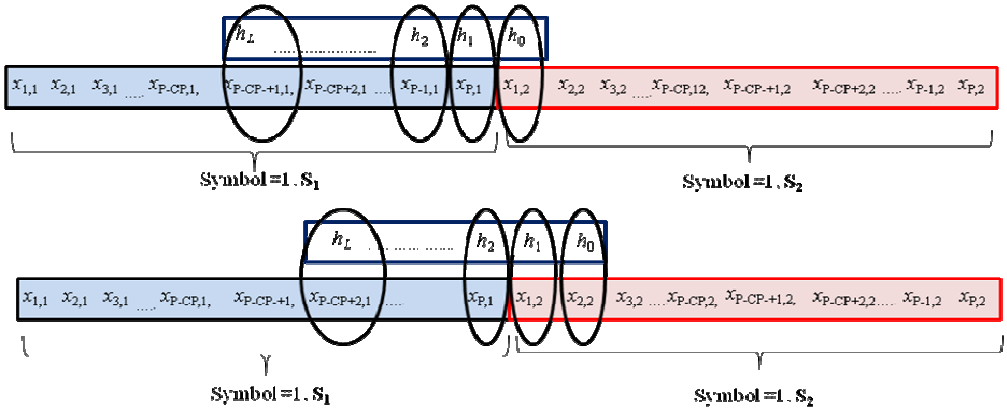

Fig. 3 The cyclic prefix creates a circular convolution at the receiver even though the actual channel causes a linear convolution.

As explained in Eq. 8 and illustrated in Fig. 3, the inter-block interference (IBI) caused by time $x_{(t-1)}$ can be eliminated by copy the last symbol of length CP and appended to the front of the block. Mathematically $\mathbf{T}_{CP}\mathbf{x}$ represents the extended SC-FDMA symbol, where $\mathbf{x}$ and $\mathbf{T}_{CP}$ are defined as follows:

$$\mathbf{T}_{CP} = \begin{bmatrix} \mathbf{0}_{CP\times(K-CP)} & \mathbf{I}_{CP\times CP} \\ & \mathbf{0}_{K\times K} \end{bmatrix} \quad (9)$$

$$\mathbf{x}_{CP} = [x_{N-CP} \quad x_{N-CP+1} \cdots \quad x_N \quad x_1 \cdots \quad x_N]^T \quad (10)$$

In SC-FDMA, the FFT output of the data symbols is mapped to a subset of subcarriers in a process known as subcarrier mapping, or subcarrier permutation. The subcarrier mapping transform matrix is denoted by $\mathbf{S}$. For each block of M data samples, $\mathbf{S}$ maps the corresponding M frequency components of the block, $\mathbf{X} = [X_0, X_1, \ldots\ldots\ldots\ldots, X_{M-1}]^T$ onto a set of M active sub-carriers selected from a total of N subcarriers, where Q' is the spreading factor, $Q' = N/M$ and $Q' > 1$. The remaining $N - M$ subcarriers are used by other uplink users. Subcarrier mapping can be classified into localized and distributed mapping, known as LFDMA and DFDMA as shown in Fig. 4. The mapping matrices for LFDMA and DFDMA are given in Eq. (11) and Eq. (12) respectively.

$$\mathbf{S} = \lfloor \mathbf{0}_{(k-1)M\times M}; \mathbf{I}_M; \mathbf{0}_{(N-kM)M} \rfloor \quad (11)$$

$$\mathbf{S} = \lfloor \mathbf{0}_{(s-1)M\times M}; (\mathbf{u}^M)^{\mathrm{T}}; \mathbf{0}_{\tilde{Q}\times M}; (\mathbf{u}^M_{s+\tilde{Q}})^{\mathrm{T}}; \ldots\ldots; \mathbf{u}^{\mathrm{T}}_{s+M\tilde{Q}}; \mathbf{0}_{(Q'-\tilde{Q})M\times M} \rfloor \quad (12)$$

where $\mathbf{u}_k^K$ denotes the unit column vector of length K, with all zero entries except at k. $\tilde{Q}$ and k denote the start of the user's subcarrier spacing for DFDMA.

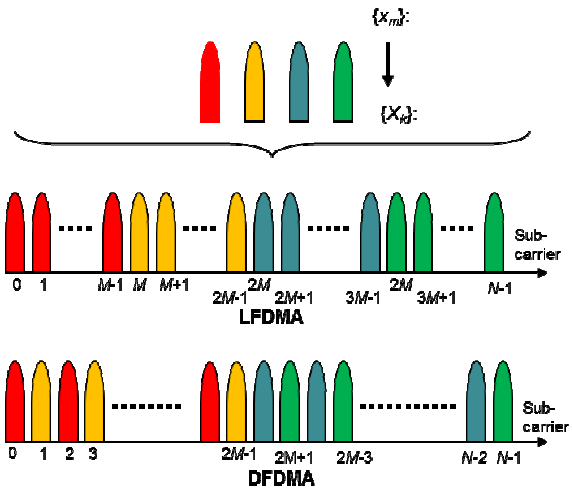

Fig. 4 An example of different subcarrier mapping modes; LFDMA, DFDMA, and IFDMA for N= 64, M = 12 with subcarrier spreading factor, Q' = 4.

At the receiver, the CP is removed following symbol synchronization. The SC-FDMA time-domain symbol is then converted into the frequency domain via an *N*-point FFT. In the demodulator, only *N* of the *M* modulated subcarriers at the output of the FFT correspond to a given user. The *N* values are then equalized (in the frequency domain) and passed through an *M*-point IFFT to recover the original data block. The IFFT matrix is denoted by $\mathbf{F}_N^{-1}$, where

$$\text{IFFT}\{S_m\} = s_n = \frac{1}{\sqrt{N}} \sum_{n=0}^{N-1} S_m e^{-j\frac{2\pi}{N}nm}. \quad (13)$$

4.0 FREQUENCY DOMAIN SPECTRUM SHAPING

The traditional time domain pulse shaping filter is used to band limit the transmit signal, whereas the frequency domain spectrum shaping process is applied to reduce PAPR. In this paper, frequency domain spectrum shaping (FDSS) is implemented in the frequency domain as shown in Fig. 5. Pulse shaping for SC-FDMA is performed using root-raised cosine (RRC) filter in the frequency domain. RRC filter is a modified type of raised cosine (RC) filter, which is derived by taking the square root of the frequency response of the raised cosine filter. It is used at both side in the transmitter and receiver of the communication systems. The mathematical equation for the frequency domain representations of RC and RRC filter is shown below in Eq. (14) and Eq. (15).

$$x_{rc}(t) = \frac{\sin \pi t / T_s}{\pi t / T_s} \frac{\cos(\pi \alpha t / T_s)}{1 - (2\alpha t / T_s)^2} \quad (14)$$

$$x_{rrc}(t) = \frac{\sin(\frac{\pi t}{\tilde{T}}(1-\alpha)) + 4\alpha \frac{t}{\tilde{T}}.\cos(\frac{\pi t}{\tilde{T}}(1+\alpha))}{\frac{\pi t}{\tilde{T}}(1 - \frac{16\alpha^2 t^2}{\tilde{T}^2})} \quad (15)$$

where $\tilde{T}$ is the symbol duration of the transmitted symbol $\tilde{x}_n$ and α is the roll-off factor.

The FFSS is implemented after the FFT and prior to the subcarrier mapping process by element-wise multiplication with the spectrum repetition of the desired pulse shaping filter. The transmit symbols in conventional single carrier (SC) systems are the actual modulated data symbols, i.e. $x_{SC}(q) = x(q)$, where q =0,1,2,.., Q−1 (assuming block-based transmission). After oversampling the transmit symbols, the peak and the output transmit signal amplitude does not diverge from the average transmit signal amplitude compare to OFDM signals. Therefore SC systems have a lower PAPR than MC systems. However, the PAPR of SC transmit signals is depend on the baseband modulation scheme, e.g. high-level QAM has higher PAPR than low-level QAM.

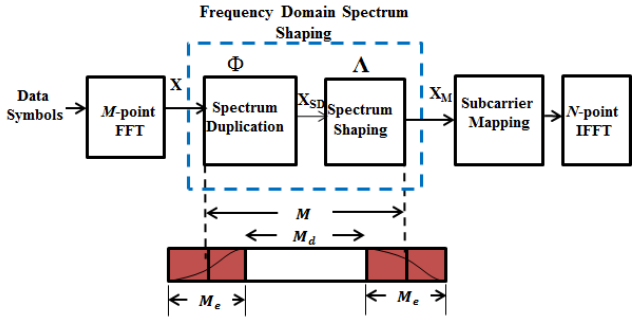

Fig.5 Pulse Shaping via Frequency Domain Spectrum Shaping

Let M_d denote the number of used subcarriers (number of data symbol) and M the number of user subcarriers, where $M \geq M_d$. The data symbols in the frequency domain are then denoted as in Eq. (16).

$$\mathbf{X} = [X_0, X_1, ..., X_{M_d-1}]^T \quad (16)$$

Prior to spectrum shaping, the frequency domain data symbols are up-sampled using a spectrum duplication block, i.e

$$\mathbf{X_{SD}} = \Phi \mathbf{X} \quad (17)$$

where Φ is a $M_d \times M$ spectrum duplication matrix given as in Eq. (18).

$$\Phi = \begin{bmatrix} 0_{M_e \times (M - M_d)} & & \mathbf{I}_{M_e} \\ & \mathbf{I}_{M_d} & \\ \mathbf{I}_{M_e} & & 0_{M_e \times (M_d - M_e)} \end{bmatrix} \quad (18)$$

where $M_e = (M - M_d)/2$. Hence the up-sampled frequency domain symbols are given by Eq. (19).

$$\mathbf{X_{SD}} = [X_{(M_d - M_e)}, ..., X_{(M_d - 1)}, X^T, X_0, ..., X_{M_e - 1}]^T \quad (19)$$

The up-sampled symbol data is filtered via frequency domain spectrum shaping using an RRC response. Let $\mathbf{\Lambda}$ denote the frequency domain spectrum shaping matrix where $\mathbf{\Lambda}$ is a $M_{sub} \times M_{sub}$ diagonal matrix with its *k*-th diagonal entry being the *k*-th spectrum shaping filter coefficient. The spectrum shaped frequency domain symbols are given by Eq. (20).

$$\mathbf{X_M} = \mathbf{\Lambda X_{SD}} \quad (20)$$

5.0 SIMULATION RESULTS AND ANALYSIS

5.1 Error Performance Results

Figs. 6a and 6b show the packet error rate (PER) performance of SISO scenario in LTE uplink for LFDMA and DFDMA SC-FDMA signal in the urban macro scenario, respectively. From the PER figures for both mapping schemes, the user will be out of service when the SNR is below 0dB while the user will be at the highest MCS approximately at 15dB and 13dB for LFDMA and DFDMA respectively (PER of 10%). It can be seen that the DFDMA outperform LFDMA for almost all modes.

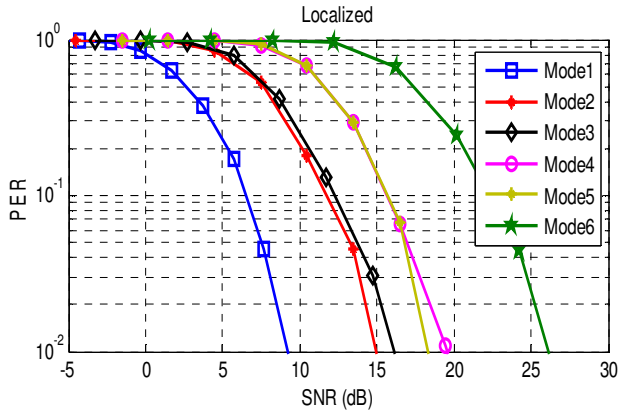

Fig. 6a PER Performance for different MCS for LFDMA.

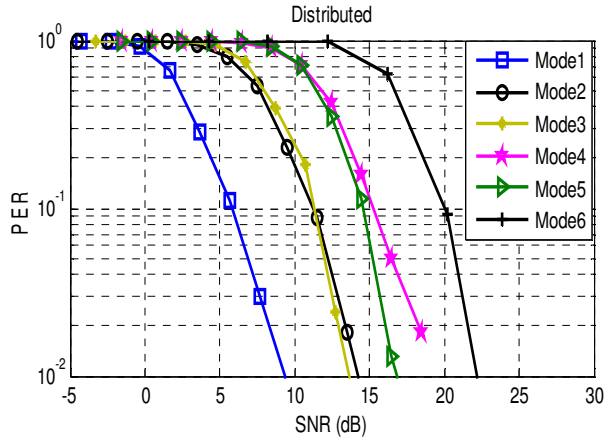

Fig. 6b PER Performance for different MCS for DFDMA.

5.2 Performance Relative to PAPR

In this paper as previously mentioned, oversampling the digital samples at the modulator output is performed via frequency domain zero-padding, and an oversampling rate of 4 is used [12]. To produce sufficiently accurate CCDF curves, 2,000 independent transmission blocks are simulated. In the following simulation, N = 1024 and M = 256 are used. For the time domain pulse shaping filter, the CCDF of the PAPR for localized and distributed SC-FDMA with different subcarrier mapping schemes using QPSK and 16QAM modulation are shown in Fig. 7.

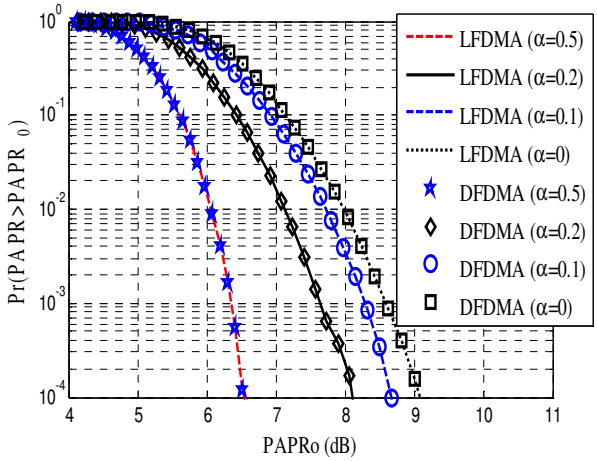

Fig. 7 PAPR comparison of LFDMA and DFDMA with 16QAM modulation using RC via FDSS at α = 0, 0.1, 0.2 and 0.5.

LFDMA is shown to have the same low-PAPR since their output transmit signals are SC signals. SC-FDMA exhibits a lower PAPR compared to OFDMA because of its single carrier structure. It also can be seen that the modulation scheme does not change the PAPR of OFDMA signals, since its high-PAPR is due to the summation of random data symbols regardless of the phase shifts (different subcarrier mapping schemes lead to different phase-shifted data symbols being summed up).

Unlike OFDMA, the PAPR of the SC-FDMA waveform is sensitive to the choice of input constellation due to the single carrier structure of SC-FDMA. The frequency-domain subcarriers in SC-FDMA are modulated by the FFT spread time-domain symbols. Hence, when the IFFT process is applied, the resulting time-domain waveform is simply an up-sampled version of the original symbol modulated sequence. Hence, the PAPR for QPSK modulated SC-FDMA is higher than 16QAM modulated SCFDMA. As LFDMA and DFDMA have the same PAPR, only the LFDMA results are shown. Although 16QAM gives higher PAPR than QPSK in LFDMA systems, 16QAM LFDMA signals still provide approximately 2dB of PAPR improvement over OFDMA signals. As in Fig. 8, LFDMA provide approximately 3.4dB and 2dB of PAPR improvement over OFDMA using QPSK and 16QAM modulation respectively. Therefore, they SC-FDMA signal is well-suited for power-efficient uplink transmission.

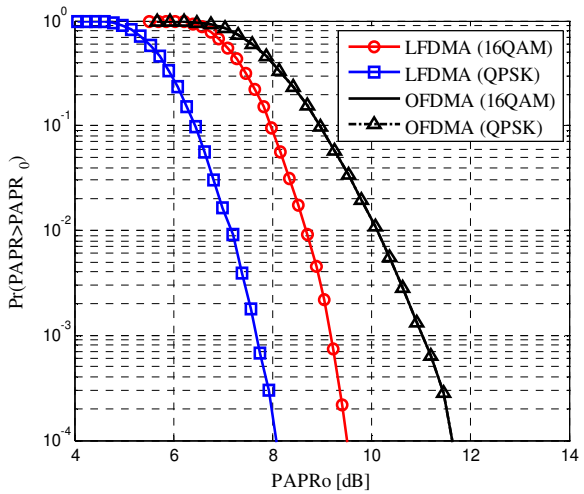

Fig. 8 PAPR comparison of LFDMA and OFDMA with QPSK and 16QAM at α=0.5.

The impact of pulse shaping is also illustrated in Fig. 9 for the case where the RC filter is implemented as a time domain signal after CP insertion and oversampling. It shows that the PAPR is reduced as the roll-off factor increases, and LFDMA and DFDMA transmit signals have the same PAPR. It is shown that the PAPR reduction for 16QAM is 6.4dB at α = 0.5. Fig. 9 compares the PAPR of LFDMA with FDSS and time domain spectrum shaping for 16QAM modulation at α=0.5 using RC pulse shaping filter. It can be seen that the LFDMA SC-FDMA signal provide approximately 2.8dB of PAPR improvement compared to LFDMA using time domain pulse shaping. The PAPR of SC-FDMA signal with RRC via FDSS is further investigated.

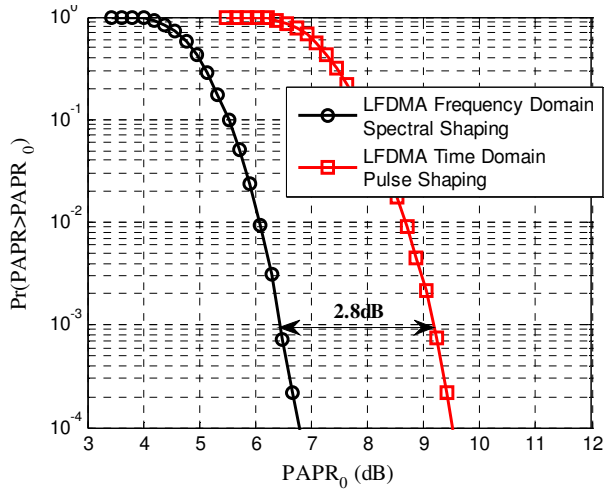

Fig. 9 PAPR of SC-FDMA for LFDMA employed RC via FDSS and time domain pulse shaping with 16QAM signaling at α = 0.5.

Fig. 10 shows the simulation results for 16QAM modulation of LFDMA when RRC via FDSS is used. It can be seen that 99.9% of LFDMA SC-FDMA transmission blocks have a PAPR less than 5.3dB. The back-off can be set to this value to ensure that the PA operates in the linear region 99.9% of time. Results have shown that a PAPR reduction of 1.9 dB can be achieved for 16QAM when RRC frequency domain spectral shaping filter with roll-off factor of 0.5 is applied.

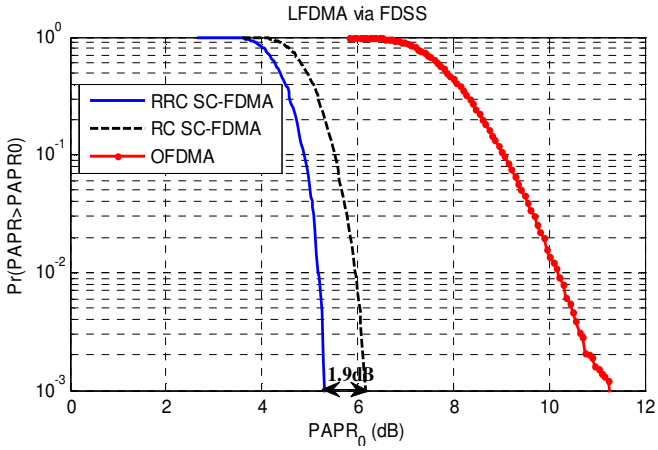

Fig.10 PAPR comparison of LFDMA SC-FDMA employed RC and RRC via FDSS with 16QAM signaling at α = 0.5.

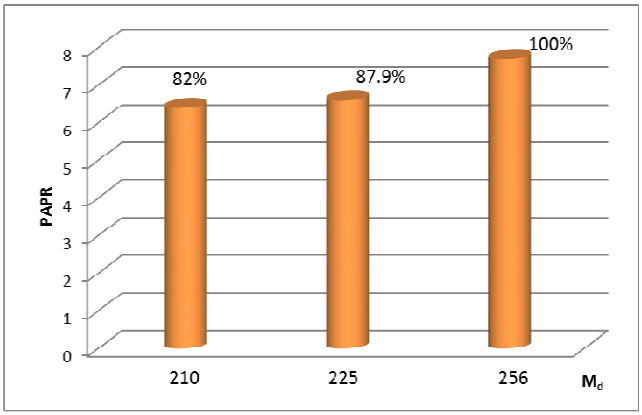

Fig. 11: Comparison of PAPR and bandwidth efficiency via RRC spectrum shaping at α = 0.5 with 16QAM modulation where the number of transmit data symbols, M_d = 210, 225 and 256.

For convenience, the PAPR results and the corresponding bandwidth efficiencies are summarized in Fig. 11. The bar chart shows the comparison of PAPR and bandwidth efficiency using RRC spectrum shaping at α = 0.5 with 16QAM modulation where the number of transmit data symbols is 210, 225 and 256 giving bandwidth efficiency of 82%, 87.9% and 100% respectively. The figure shows that the bandwidth efficiency is increased as the PAPR increases.

6.0 CONCLUSIONS

The interrelationship between PAPR, bandwidth efficiency, probability of bit error and packet error rate has been presented. Performance results have been analyzed for 3GPP LTE standard and for all transmission modes for the case of transmission over SCME channel. There is a difference between the time domain pulse shaping used in traditional single carrier systems and the frequency domain spectrum shaping used in SC-FDMA. For frequency domain SC-FDMA signals the abrupt discontinuity at the spectrum edges gives rise to a large variation in the continuous transmits signal waveform. The use of additional subcarriers to smooth the transition bandwidth through frequency domain spectrum shaping has been shown to smooth the transmit signal waveform. The resulting PAPR reduction can be used to enhance handset power efficiency, or alternatively to improve uplink throughput and/or operating range. Hence, the results show that a tradeoff exists between PAPR and bandwidth efficiency making the choice of filter and radio resource algorithm critical in SC-FDMA systems such as LTE.

REFERENCES

[1] Mustafa Ergen, 'Mobile Broadband: Including WiMAX and LTE', Berkeley, CA, USA, *Springer-Verlag*, 2009.

[2] Toskala, A, Holma, H., Pajukoski, K., Tiirola, E., 'UTRAN Long Term Evolution in 3GPP'. *The 17th Annual IEEE International Symposium on Personal, Indoor and Mobile Radio Communications (PIMRC '06),* in Proceedings, 2006, Helsinki, Finland.

[3] NTT DoCoMo, NEC, and SHARP, 'R1-050702: DFT-spread OFDM with Pulse Shaping Filter in Frequency Domain in Evolved UTRA Uplink', www.3gpp.org, *3GPP TSG RAN WG1*, meeting 42, London, UK, August 2005.

[4] A. S Kang, Vishal Sharma,'Pulse Shape Filtering in Wireless Communication-A Critical Analysis', (IJACSA) International Journal of Advanced Computer Science and Applications, Vol. 2, No.3, March 2011.

[5] H.G. Myung, J. Lim, and D.J. Goodman. 'Peak-to-Average Power Ratio of Single Carrier FDMA Signals with Pulse Shaping', *Proc. of the IEEE PIMRC*, pp. 1-5. Sep. 2006.

[6] G. Huang, A. Nix, and S. Armour. 'Impact of Radio resource allocation and Pulse shaping on PAPR of SC-FDMA signals', *PIMRC*-07, 2007.

[7] D. Falconer, S. L. Ariyaritakul, A. Benyamin-Seeyar, and B. Eidson, "Frequency Domain Equalization for Single-Carrier Broadband Wireless Systems," *IEEE Commun. Mag*., vol. 40, no. 4, Apr. 2002, pp. 58-66.

[8] Yang Li; Zhu, R.; Prikhodko, D.; Tkachenko, Y.; , "LTE power amplifier module design: Challenges and trends," Solid-State and Integrated Circuit Technology (ICSICT), pp.192-195, 1-4 Nov., 2010.

[9] 3GPP TSG-RAN-WGI, "Evolved Universal Terrestrials Radio Access (E-UTRA): Further Advancements for E-UTRA Physical Layer Aspects," 3GPP, Tech. Rep. TR 36.814, 2010.

[10] "Technical Specification Group Radio Access Network, Physical channels and modulation." *3GPP TS 36.211 V8.1.0* Nov. 2007.

[11] White Paper, "Global Mobile Data Traffic Forecast Update, 2009-2014", Cisco Visual Networking Index, 2010-02.

[12] S. Han and J. Lee, "An Overview of Peak-to-Average Power Ratio Reduction Techniques for Multicarrier Transmission," *IEEE Wireless Communications*, vol. 12, pp. 56-65, April 2005.

[13] J.G. Proakis, *Digital Communications*, 4th Ed., McGraw-Hill, 2001.

[14] Akter R, Islam MR, Song JB., 'PAPR in 3 rd Generation Partnership Project Long Term Evolution: An Overview to Find the Impact', IETE Tech Rev.

[15] Huawei, 'R1-051434: Optimum family of spectrum-shaping functions for PAPR reduction in SC-FDMA', www.3gpp.org, 3GPP TSG RAN WGI, meeting 43, Seoul, Korea, November 2005.